

Wavelength scanning digital interference holography for variable tomographic scanning

Lingfeng Yu and Myung K. Kim

Dept. of Physics, University of South Florida, Tampa, FL 33620
yulingfeng@gmail.com, mkkim@cas.usf.edu

Abstract: We present a novel technique of variable tomographic scanning capable of reconstructing tomographic images of an object volume along any arbitrarily tilted plane. The method is based on wavelength scanning digital interference holography, using a series of holograms generated with a range of scanned wavelengths. From each hologram, the object field is reconstructed in a number of selected tilted planes. The desired tomographic images are then reconstructed from the numerical superposition of the object fields. Thus the tomographic images can be generated along variable planes without the need for physically repeating the scanning and recording processes. Experimental results are presented to verify the proposed concept.

©2005 Optical Society of America

OCIS codes: (090.1760) Computer holography; (110.6880) Three-dimensional image acquisition; (180.0180) Microscopy

References and links

1. D.Huang, E.A.Swanson, C.P.Lin, J.S.Schuman, W.G.Stinson, W.Chang, M.R.Hee, T.Flotte, K. Gregory, C.A.Puliafito, and J.G.Fujimoto, "Optical coherence tomography," *Science* **254**, 1178-1181 (1991).
2. B. Laude, A. De Martino, B. Drevillon, L. Benattar, and L. Schwartz, "Full-field optical coherence tomography with thermal light," *Appl. Opt.* **41**, 6637-6645 (2002).
3. L. Yu and M. K. Kim, "Full-color three-dimensional microscopy by wide-field optical coherence tomography," *Opt. Express* **12**, 6632-6641 (2004), <http://www.opticsexpress.org/abstract.cfm?URI=OPEX-12-26-6632>.
4. A. Dubois, K. Grieve, G. Moneron, R. Lecaque, L. Vabre, C. Boccara, "Ultrahigh-Resolution Full-Field Optical Coherence Tomography," *Appl. Opt.* **43**, 2874-2883 (2004).
5. G. Pedrini and H.J. Tiziani, "Short-coherence digital holography by use of a lensless holographic imaging system," *Appl. Opt.* **41**, 4489-4496 (2002).
6. M.K. Kim, "Tomographic three-dimensional imaging of a biological specimen using wavelength-scanning digital interference holography," *Opt. Express* **7**, 305-310 (2000), <http://www.opticsexpress.org/abstract.cfm?URI=OPEX-7-9-305>.
7. M.K. Kim, "Wavelength-scanning digital interference holography for optical section imaging," *Opt. Lett.* **24**, 1693-1695 (1999).
8. J. W. Goodman. *Introduction to Fourier Optics*. McGraw-Hill, 1996.
9. D. Leseberg and C. Frere, "Computer-generated holograms of 3-D objects composed of tilted planar segments," *Appl. Opt.* **27**, 3020-24 (1988).
10. L. Yu, Y. An, and L. Cai, "Numerical reconstruction of digital holograms with variable viewing angles," *Opt. Express* **10**, 1250-1257, (2002), <http://www.opticsexpress.org/abstract.cfm?URI=OPEX-10-22-1250>.
11. P. Ferraro, S.De Nicola, G. Coppola, A. Finizio, D. Alfieri, G. Pierattini, "Controlling image size as a function of distance and wavelength in Fresnel-transform reconstruction of digital holograms," *Opt. Lett.* **29**, 854-856 (2004).
12. O. Schnars and W. Juptner, "Direct recording of holograms by a CCD target and numerical reconstruction," *Appl. Opt.* **33**, 179-181 (1994).

1. Introduction

Three-dimensional microscopic imaging that reveals the tomographic structure of biological tissues or other materials has a variety of applications in clinical and laboratory studies. Recently developed optical coherence tomography [1] (OCT) is a scanning microscopic technique that is suitable for high-resolution cross-sectional imaging, which uses a Michelson-Type interferometer and is designed to detect a heterodyne signal in the interference of the back-scattered light from the sample point and the reference mirror. The three-dimensional image is reconstructed by scanning the three dimensions pixel by pixel. Its axial and lateral resolutions are determined by the source coherence length and the numerical aperture of the sampling lens, respectively. Since parallel acquisition of two-dimensional images while maintaining the optical sectioning characteristics of OCT would have obvious attractions, full-field OCT techniques [2-4] have also been reported to acquire the two-dimensional tomographic images. A related technique, short-coherence digital holography [5] is used for three-dimensional microscopic investigations, where a short-coherence laser is used as the light source to record the holograms on a CCD sensor. The image of the part of the sample that matches the reference mirror distance within the coherence length is reconstructed by numerical evaluation of the hologram. The 3D microscopic structure of a specimen can be successfully reconstructed by scanning a reference mirror with a fixed orientation. Another 3D microscopy and tomographic imaging system that we have been developing is the wavelength-scanning digital interference holography (WSDIH) [6,7], where a series of holograms are recorded using a range of scanned wavelengths. The image volume is calculated from each of the holograms and all such image volumes are numerically superposed to create the 3D tomographic image. The process results in a synthesized short coherence length and corresponding axial resolution. The plane on which the reference mirror is located is called the scanning plane and its normal direction is defined as the scanning direction in this paper.

In most of the 3D microscopy systems including the OCT and the WSDIH, the 3D volume is reconstructed as a set of scanning planes with the scanning direction along the optical axis of the system. If a tomographic image on a plane not parallel to the original reference mirror is required, it can be reconstructed by combining or interpolating points from different tomographic layers, however the quality will be degraded, especially when the lateral resolution does not match well with the axial resolution. In order to get better results, the whole process needs to be physically repeated with the reference mirror tilted or the object rotated to a desired orientation.

In this paper we propose a novel technique that is capable of variable tomographic scanning with flexible selection of scanning planes without physically repeating the scanning or recording process. The system is based on the principle of wavelength scanning digital interference holography. The tomographic images reported in Refs. [6] and [7] are all obtained with a fixed scanning direction parallel to the optical axis of the system. Since the advantage of digital holography is that a single hologram records the entire three-dimensional information of the object, the object wave distributions and the synthesized tomographic image at an arbitrarily tilted plane can be reconstructed rigorously, and selective tomographic scanning with different orientation is possible. This tilted reconstruction plane then functions as the scanning plane in the WSDIH.

2. Principle

Suppose an extended object is illuminated by a laser beam of wavelength λ . The scattered wave from any point P of the object (at \mathbf{r}_p) can be viewed as a Huygens wavelet, so that the resultant field $E(\mathbf{r})$ at \mathbf{r} is

$$E(\mathbf{r}) \sim \int A(\mathbf{r}_p) \exp(ik|\mathbf{r} - \mathbf{r}_p|) d^3\mathbf{r}_p, \quad (1)$$

where $A(\mathbf{r}_p)$ is proportional to the amplitude and phase of a wavelet scattered from the point \mathbf{r}_p , and the integral is over the object volume. Here we have neglected the $1/r$ wavelet amplitude dependence as approximately constant over \mathbf{r}_p . The amplitude and phase of this field at the hologram plane $z = 0$ is recorded by the hologram. If the holographic process is repeated using a range of scanned wavelengths, and the reconstructed fields are all superposed together, then the resultant field is

$$E(\mathbf{r}) \sim \sum_k \int A(\mathbf{r}_p) \exp(ik|\mathbf{r}-\mathbf{r}_p|) d^3\mathbf{r}_p \sim \int A(\mathbf{r}_p) \delta(\mathbf{r}-\mathbf{r}_p) d^3\mathbf{r}_p \sim A(\mathbf{r}), \quad (2)$$

which is proportional to the field at the object and is nonzero only at the object points. In practice, if one uses a finite number N of wavelengths at regular intervals of $\Delta(1/\lambda)$, then the object image $A(\mathbf{r})$ repeats itself (other than the diffraction/defocusing effect of propagation) at a beat wavelength $\Lambda = [\Delta(1/\lambda)]^{-1}$, with axial resolution $\delta = \Lambda/N$. By use of appropriate values of $\Delta(1/\lambda)$ and N , the beat wavelength Λ can be matched to the axial extent of the object, and δ to the desired level of axial resolution.

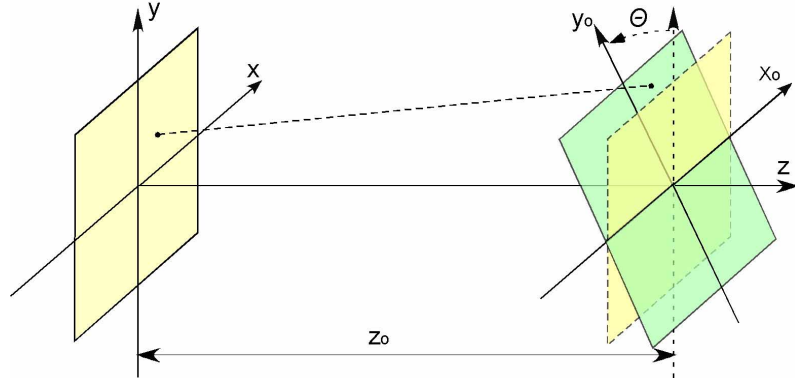


Fig. 1. Reconstruction of the wavefield on a tilted $x_o - y_o$ plane for a given wave distribution on the x - y plane (hologram plane). See text for details.

Diffraction from a tilted plane based on the Rayleigh-Sommerfeld diffraction formula [8] was previously studied for computer-generated holograms [9] by D. Leseberg *et al*, and was later applied for numerical reconstruction of digital holography with changing viewing angles [10]. In this paper we will extend the algorithm to consider a slightly different situation, reconstructing the wave distribution in a variable tilted plane. Suppose the object wave distribution $o(x, y)$ on the hologram (at the $z=0$ plane) is already known. For simplicity, reconstruction of the wave distribution on a tilted plane, $x_o - y_o$, with its normal in y - z plane is considered, as shown in Fig. 1. The Rayleigh-Sommerfeld diffraction integral gives:

$$E(x_o, y_o, z_o) = \frac{iE_0}{\lambda} \iint o(x, y) \frac{\exp[ikr(x, y, x_o, y_o)]}{r(x, y, x_o, y_o)} \chi(x, y, x_o, y_o) dx dy, \quad (3)$$

where k is the wave number given by $k = 2\pi/\lambda$. E_0 is a constant and $\chi(x, y, x_o, y_o)$ is the inclination factor, which is approximately unitary under the Fresnel approximation and is omitted from the following equations. The inverse length $1/r$ can be replaced by $1/r_o$ and the $r(x, y, x_o, y_o)$ in the argument of the exponential can be expressed as:

$$r = \sqrt{(z_o - y_o \sin \theta)^2 + (x - x_o)^2 + (y - y_o \cos \theta)^2}, \quad (4)$$

which can be expanded as a power series of $r_o = (z_o^2 + x_o^2 + y_o^2)^{1/2}$. If only the first two lowest order terms in the expanded series are considered, and a further approximation is introduced, $ik(x^2 + y^2)/2r_o \approx ik(x^2 + y^2)/2z_o$, which holds almost the same restriction as the Fresnel condition, Eq. (3) can be finally expressed as:

$$E(\xi, \eta, z_o) = \frac{iE_0}{\lambda r_o} \exp \left[ik \left(r_o - \frac{z_o y_o \sin \theta}{r_o} \right) \right] \times \iint o(x, y) \exp \left[\frac{ik}{2z_o} (x^2 + y^2) \right] \exp[-i2\pi(\xi x + \eta y)] dx dy, \quad (5)$$

with:

$$\xi = \frac{x_o}{\lambda r_o}, \text{ and } \eta = \frac{y_o \cos \theta}{\lambda r_o}. \quad (6)$$

Equation (5) can be implemented with the fast Fourier transform (FFT) algorithm and a coordinate transform is made to get the wave distribution in the (x_o, y_o) coordinate as indicated in Eq. (6).

In the discrete implementation of Eq. (5), the resolution of the reconstructed plane is determined according to the Shannon theory, and is given approximately as:

$$\Delta x_o = \frac{\lambda z}{N \Delta x}, \quad \Delta y_o = \frac{\lambda z}{N \Delta y \cos \theta} \quad (7)$$

where Δx_o and Δy_o are the resolutions of the tilted plane, Δx and Δy are the resolutions of the hologram plane and $N \times N$ is the array size of a square area on the CCD. In order to keep the reconstructed resolution consistent at different z planes, a zero-padding method [11] can be used by simple padding of the recorded hologram with zeros in both the horizontal and vertical directions. Note that if the tilted angle θ is equal to zero, then Eq. (5) simplifies to the well-known Fresnel diffraction formula [12]. Although the above algorithm only considers the situation that the angle θ lies in the y - z plane, it can easily be extended to any tilted angle θ in space. From the above, the wave fields at an arbitrarily tilted plane can be reconstructed from the holograms, and the tomographic images in WSDIH, synthesized from multiple wave distributions, can be flexibly adjusted to variable orientations.

3. Experiments

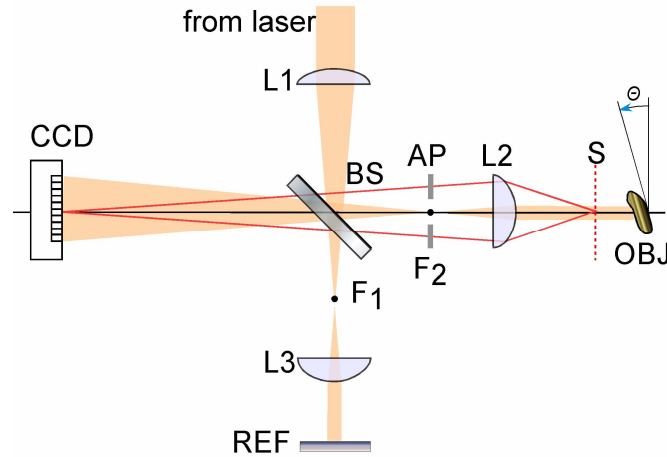


Fig. 2. Optical apparatus used in the digital interference holography experiments. The Ls are various lenses; BS is a beamsplitter; AP is an aperture and REF is a mirror. The CCD camera captures the interference pattern at the plane S.

Experiments are performed to verify the effectiveness of the proposed idea. Figure 2. shows the optical setup of the WSDIH system using a Michelson interferometer illuminated by a Coherent 699 ring dye laser, which can be tuned continuously from 567.0 nm to 613.0 nm. The lens $L1$ provides plane-wave illumination of the object by focusing the input laser at the front focus of $L2$. The plane S is imaged to the CCD camera by the lens $L2$. Collimating the reference beam with $L3$ then results in a magnified image at the CCD camera of an interference pattern that would exist at S if the object wave is superposed with a plane wave there. An aperture is placed in the focal plane of $L2$ to control the size of the object spectrum captured in the CCD camera. The object and the reference beams are tilted with respect to each other in an off-axis hologram arrangement. The object angular spectrum can be separated from other spectral components of the hologram with a band-pass filter if the off-axis angle of the incident beam is properly adjusted. Then, the pure object wave distribution $o(x, y)$ on the hologram plane can be readily extracted by taking an inverse Fourier transform of the object spectrum.

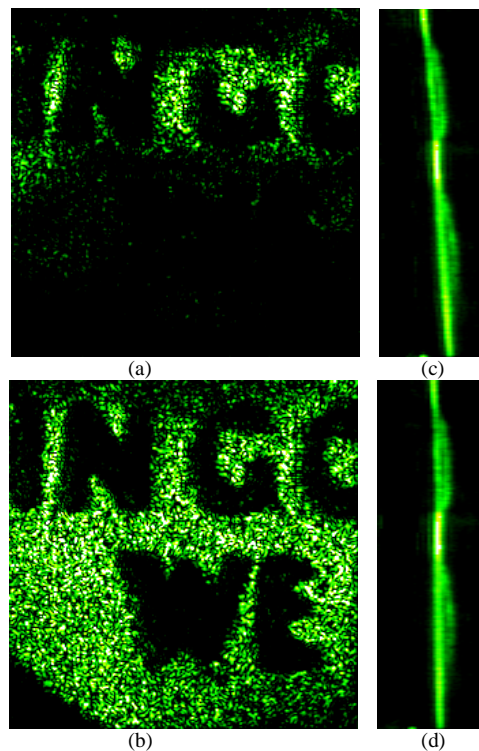


Fig. 3. Contour images of a dime in a $2.25 \times 2.25 \times 0.6 \text{ mm}^3$ volume: (a) (QuickTime, 1.40MB) The animation shows x_o - y_o cross sections with normal tomographic scanning by the Fresnel diffraction formula; (b) (QuickTime, 0.98MB) The animation shows x_o - y_o cross sections with tilted tomographic scanning by the proposed algorithm; (c) and (d) are flat views of the y_o - z cross sections from (a) and (b).

In our experiment, the WSDIH system images a surface area of a dime, $2.25 \times 2.25 \text{ mm}^2$, 256×256 pixels, which is slightly tilted with a small angle $\theta = 3^\circ$ to the hologram plane, as shown in Fig. 2. The reconstruction distance z , representing the distance from the object to S plane in Fig. 2 is set to be 35 mm. The wavelengths of the dye laser is scanned for a range of 575.0 to 585.0 nm at 20 values (19 equal increments of $1/\lambda$), which gives an axial range of $\Lambda = 639 \text{ }\mu\text{m}$ and axial resolution of $\delta = 32 \text{ }\mu\text{m}$. The lateral resolution is the same as the reconstruction resolution defined in Eq. (7) and is about $9 \text{ }\mu\text{m} \times 9 \text{ }\mu\text{m}$ in the experiment. For comparison, the Fresnel Diffraction formula is used first to reconstruct the wave fields for

scanning direction normal to the hologram plane. The wave distributions from all the holograms are numerically superposed together to obtain the accumulated field distribution that represents the three dimensional object structure. Figure 3(a) shows an animation of scanning a sequence of contour images at different layers of the object at $15\ \mu\text{m}$ axial distance intervals. Since the coin is slightly tilted relative to the hologram plane, the contour images sequentially appear from bottom to top in Fig. 3(a) as the distance z is increased. The scanning planes can be selectively adjusted by using the reconstruction algorithm proposed above, and they are now set parallel to the base surface of the coin, so that the features of the relief appear simultaneously in a single tomographic scanning. Specifically, in our experiment the tilted angle of the reconstruction plane is set to be $\theta = 3^\circ$, as shown in Fig. 1. Figure 3(b) shows a demo of tilted tomographic scanning that the letters on the coin are now either all highlighted or all darkened, for they are located in the same scanning plane. Figure 3(c) is the flat view of all the y_o - z cross sections from 3(a), which clearly shows a tilted angle between the coin base surface and the scanning plane. Similarly, the y_o - z flat view for the tilted tomographic scanning is shown in Fig. 3(d), the scanning plane is now parallel to coin base surface and shown vertical in the picture.

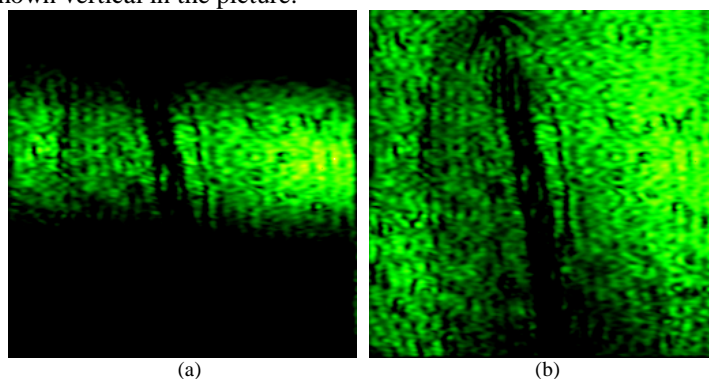


Fig. 4. Contour images of a chick embryo in a $2.26 \times 2.26\ \text{mm}^2$ area: (a) (QuickTime, 1.12MB) The animation shows normal tomographic scanning with the Fresnel diffraction formula; (b) (QuickTime, 1.12MB) The animation shows tilted tomographic scanning with the proposed algorithm.

Figure 4 shows another example of a prepared slide of a chick embryo, of area $2.26 \times 2.26\ \text{mm}^2$. The embryonic blood vessel is located in a tilted plane with $\theta = 2.5^\circ$. Figure 4(a) shows the tomographic images with normal scanning. If the scanning plane is intentionally tilted with a proper angle of $\theta = 2.5^\circ$ however, the whole blood vessel is reconstructed at one tomographic image as shown in Fig. 4(b). Although the objects in the experiments are tilted with relatively small angles of θ , the proposed algorithm can provide good reconstructions for tilted angles θ up to ± 60 degrees, according to numerical analysis for this case. Theoretically, the Fresnel approximate conditions will impose a restriction to the extent of the titled plane, which is related to the tilted angle. Furthermore, bigger tilted angle will induce a larger reconstructed pixel resolution of the tilted plane, as indicated in Eq. (6). Thus we intend to select tilted angles smaller than 60 degrees in our experiment.

As we can see from the above two examples, the proposed algorithm can be used to better observe interesting structures or features randomly oriented on planes that are not parallel to the original scanning plane. Although the 3D volume can be reconstructed as a set of scanning planes perpendicular to the optical axis, and a tilted tomographic image can be obtained by combining or interpolating points from different tomographic layers, however, the quality of the interpolated image will be greatly degraded if the lateral resolution does not match well with the axial resolution. The intention of this paper is to calculate more rigorous wavefield distributions on a titled plane directly from the recorded holograms, since the advantage of digital holography is that the holograms have recorded all the information of the object, and

the synthesized tilted tomographic images will have better quality than those only from interpolation. Although the current method introduces some approximate conditions and uses coordinate transform as well, it will be our future work to develop or try more rigorous algorithms for tilted reconstructions.

At this stage of development, the need to manually scan the laser wavelength limits the acquisition time, which can be greatly accelerated if motorized micrometer under computer control is used for scanning in the near future. Then the limiting factor will be the camera frame rate. The sensitivity of the WSDIH system is mainly limited by the electronic noise of the camera and the dynamic range of the CCD sensor, and is approximately 60 dB in our system. It can be highly improved by using a CCD camera with higher dynamic range or incorporating binning or image lock-in techniques.

4. Conclusion

In conclusion, the above experiment clearly shows that variable tomographic scanning is possible in WSDIH, given that the holograms contain all the information of the three-dimensional object that is necessary for numerical reconstruction. By reconstructing the wave distribution in an arbitrarily tilted plane, which functions as the scanning plane in WSDIH, the tomographic image can be reconstructed accordingly. Although the examples presented only show the surface profile of the dime or a thin object, the capability of WSDIH to generate cross-sectional views of sub-surface structure has been experimentally demonstrated [6]. This technique will be very useful for acquiring and observing images of randomly orientated features of a specimen in a WSDIH system.

The authors thank Prof. S.K. Pierce for providing the chick embryo sample, and Leo Krzewina for helpful discussions. They gratefully acknowledge the financial support of the National Science Foundation.